Available online at www.sciencedirect.com
SCIENCE DIRECT
Journal of Photochemistry and Photobiology A: Chemistry 182 (2006) 107–111
Journal of Photochemistry and Photobiology A:Chemistry
www.elsevier.com/locate/jphotochem

Short note

UV laser co-photolytic gas-phase formation and deposition of nano-sized germanium sulfides

Radmila Tomovska [a], Vladimír Vorlíček [b], Jaroslav Boháček [c], Jan Šubrt [c], Josef Pola [a,*]

[a] *Laboratory of Laser Chemistry, Institute of Chemical Process Fundamentals, Academy of Sciences of the Czech Republic, 165 02 Prague, Czech Republic*
[b] *Institute of Physics, Academy of Sciences of the Czech Republic, 18040 Prague, Czech Republic*
[c] *Institute of Inorganic Chemistry, Academy of Sciences of the Czech Republic, 25068 Řež, Czech Republic*

Abstract

ArF laser co-photolysis of gaseous tetramethylgermane–thiirane mixtures results in chemical vapour deposition of nano-sized germanium sulfides (GeS and GeS_2) whose formation is explained by gas-phase reaction between transiently formed nanosized clusters of S and Ge atoms. Other photolytic channels allow formation of S- and Ge-containing polymers.

Keywords: Laser co-photolysis; Tetramethylgermane; Thiirane; Nanoparticles; Germanium sulfides

1. Introduction

In recent years, nanostructured films and nanoparticles of metal chalcogenides have been the subject of growing interest because of their outstanding electronic and optical properties. Among the variety of these compounds, a great attention has been paid to nanostructured films for e.g., [1] and nanoparticles [2] of binary Ag, Cd and Zn sulfides. As for the nanosized sulfides of the 4B group elements (Si, Ge, Sn, Pb), considerable attention was given only to nanoscopic sulfides of lead [3] and tin [4]. Surprisingly, no synthesis of crystalline or amorphous nanosulfides of germanium have yet been reported, despite that germanium sulfide glasses for e.g., [5] and films for e.g., [6] are of great importance because of their switching and memory properties.

We have previously reported [4c] on chemical vapour deposition of nanosized tin sulfides, accomplished through simultaneous, laser-induced generation and reaction of Sn and S clusters in the gas phase. In this process Sn and S clusters were obtained by UV laser co-photolysis of tetramethyltin and carbon disulfide and the deposited SnS and SnS_2 nanoparticles were incorporated in a polymer framework.

In this work we show that the technique of simultaneous laser irradiation of two progenitors leading [7] to generation of two different elements and to their reaction in the gas phase can be applied to gas-phase synthesis of nanostructured germanium sulfides. It is known that (i) ArF laser photolysis of gaseous thiirane (c-C_2H_4S) is dominated [8] by a channel yielding sulfur atoms and ethene and can serve as a route to gas-phase S atoms and that (ii) the ArF laser photolysis of gaseous tetramethylgermane TMG leads to almost complete stripping of organic substituents from germanium, allows deposition of Ge (major product) along with an organogermanium polymer (minor product) and is suitable for gas-phase generation of Ge cluster [9].

We laser-photolysed gaseous c-C_2H_4S–TMG mixtures, examined the obtained solid products by X-ray photoelectron spectroscopy, Raman spectroscopy, infrared spectroscopy and electron microscopy and report on the first gas-phase synthesis and chemical vapour deposition of nanosized germanium sulfides.

2. Experimental

The ArF laser co-photolysis of gaseous thiirane (10 Torr)–TMG (10, 20 and 50 Torr) mixtures, and of each of the constituent alone (20 Torr), was conducted at room temperature using an ELI 94 laser operating at 193 nm with a pulse energy of 60 mJ and repetition frequency of 10 Hz. The laser beam was mildly focused to achieve incident fluences of 150 mJ cm^{-2} and to avoid dielectric breakdown. The gaseous samplers were irradiated in a Pyrex reactor (base pressure less

* Corresponding author. Tel.: +420 2 20390308; fax: +420 2 20920661.
E-mail address: pola@icpf.cas.cz (J. Pola).

1010-6030/$ – see front matter © 2006 Elsevier B.V. All rights reserved.
doi:10.1016/j.jphotochem.2006.05.006

than 0.07 Torr, 140 ml in volume, two orthogonally positioned tubes, one fitted with two KBr windows and the other furnished with two quartz plates), which was equipped with a sleeve with a rubber septum and PTFE valve connecting it to a vacuum-line. It accommodated Au, KBr and quartz substrates, which, covered with the deposited solid material in the course of photolysis, were transferred for the Raman, UV/VIS and electron microscopy measurements. (The FTIR spectra of the deposited solids were measured directly in the reactor after prolonged evacuation of the reactor).

The progress of the photolysis was monitored by periodically removing the reactor from the laser irradiation section and placing it in the compartment of an FTIR (Nicolet Impact 400) spectrometer. The depletion of thiirane and TMG was, respectively determined using analytical bands at 627 and 1244 cm^{-1}. The volatile products of the photolysis were analysed by FTIR spectroscopy, GC-MS (a QP 1000 Shimadzu mass spectrometer) and their relative yields were determined by gas chromatography (a Shimadzu GC 14A chromatograph, FID detector, a Chromatopac C-R5A computing integrator). Both instruments were equipped with Porapak P (1.5 m long) columns and operated at programmed temperature (30–150 °C) with He carrier gas.

The Raman spectra were measured on a Renishaw (a Ramascope model 1000) Raman microscope coupled with a CCD detector. The exciting beam of an Ar ion laser was defocused to obtain an energy density of ca. 350 W cm^{-2}.

SEM images were acquired using a Philips XL30 CP scanning electron microscope. TEM analysis (particle size and phase analysis) was carried out on a Philips 201 transmission electron microscope at 80 kV on deposited materials scraped from the Au surface and transferred to a Formvar 1595 E (Merck) membrane-coated Cu grid. Process diffraction [10] was used to evaluate and compare measured electron diffraction patterns with an XRD diffraction database [11].

Thiirane and tetramethylgermane (both Aldrich) were distilled prior to use.

3. Results and discussion

3.1. Photolytic features

The ArF laser co-photolysis of gaseous thiirane (10 Torr) –TMG (10, 20 and 50 Torr) mixtures results in depletion of both compounds and the formation of volatile hydrocarbons (mainly CH_4, C_2H_4 and C_2H_6 along with small amounts of C_2H_2 and traces of C_3 and C_4 hydrocarbons). A fog is produced simultaneously and slowly descending onto the reactor bottom as an ultrafine powder to produce thin films.

The distribution of the main hydrocarbons is affected with the thiirane/TMG initial ratio (r) [(in relative mole% for $r = 1$, 0.5 and 0.2): CH_4 (14, 18, 25), C_2H_4 (68, 56, 41) and C_2H_6 (14, 18, 20)] and so is the color of the formed fog and of the deposited solid material, which is whitish-grey ($r = 0.2$ and 0.5) or clearly dark-red ($r = 1$).

We note that an independent ArF laser photolysis at the same irradiation conditions of thiirane (a major channel [8] yielding sulfur atoms and ethene) gives ethene (a far major product) and

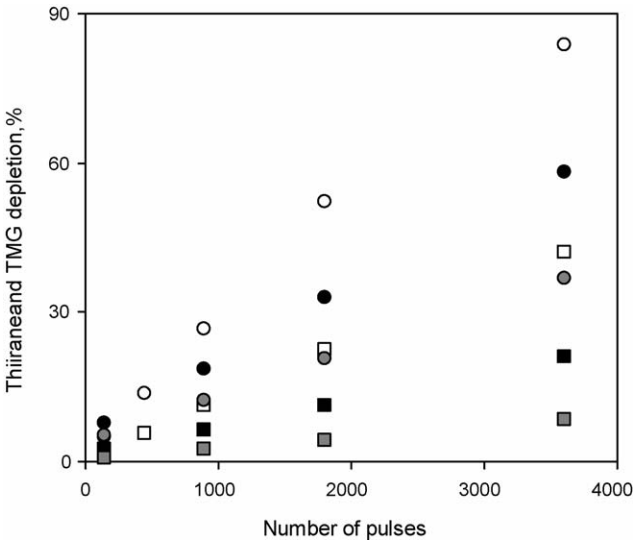

Fig. 1. Thiirane and TMG depletion as dependent on number of pulses. Circles (thiirane) and squares (TMG) are empty ($r = 1$), full ($r = 0.5$) and shadowed ($r = 0.2$).

H_2S and CS_2 (minor products). That of TMG (occurring [9] as a sequence of radical and molecular steps [9b] producing mostly neat Ge and some organogermanium polymer) leads to the formation of methane, ethane (both ca. 40–45 mole%) and ethene (ca. 15 mole%) and traces of ethyne.

The energy delivered by 193 nm photons (corresponding to ca. 620 kJ $mole^{-1}$) is in excess of the energy needed for the cleavage of both Ge–C (ca. 240 kJ $mole^{-1}$) [12] and C–S (thiirane [13], ca. 215 kJ $mole^{-1}$) bonds and the gaseous products (the absence of large amounts of propene) are in line with virtually non-interfering ArF laser–induced decompositions of both constituents.

Thiirane depletes more efficiently than TMG (Fig. 1), which is due to (i) higher absorptivity of thiirane [at 193 nm in 10^{-2} $Torr^{-1}$ cm^{-1}: 4.7 (thiirane) and 2.3 (TMG)] and partly (ii) lower bond dissociation energy of the C–S compared to the C–Ge bond. The more feasible photolysis of thiirane supplies, in principle, the gas phase with more elemental S than elemental Ge, which is in accord with the fewer bonds to be cleaved to produce elemental S than elemental Ge. The assumed proportion of the neat Ge in the gas phase can be increased at lower r (Fig. 1) when amount of decomposed TMG molecules increases.

3.2. Properties of solid deposits

The SEM images of the solid deposits differ at $r = 1$, 0.5 and 0.2 only slightly. The illustrative comparison of the solids obtained by the irradiation of the mixtures and separate thiirane and TMG (Fig. 2) reveals that all the solids consist of ca. 10–20 μm sized agglomerates.

The EDX-SEM analyses of the solid from TMG ($Ge_{1.00}C_{0.60}O_{0.20}$) and that from thiirane ($C_{1.00}S_{0.26}O_{0.02}$) are in keeping with rather significant incorporation of oxygen into the framework of the Ge/C material and a very small uptake of O by a polymer obtained from thiirane. The S content in the

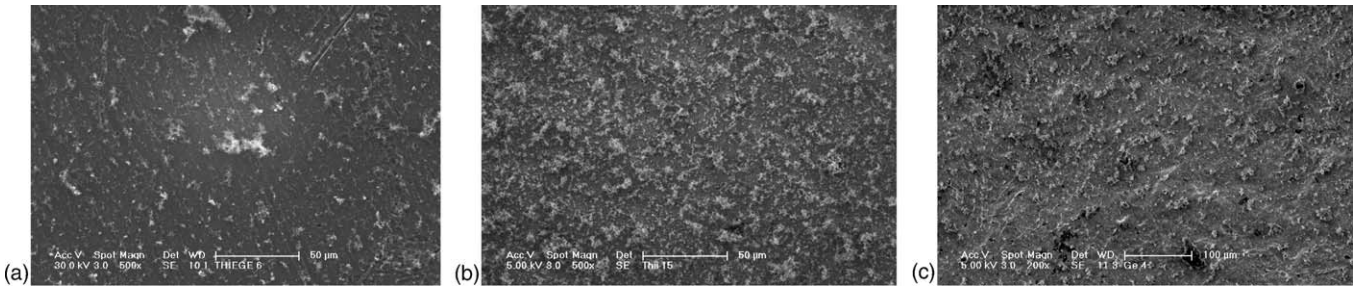

Fig. 2. SEM images of deposits obtained from equimolar mixture of thiirane and TMG (a), thiirane (b), and TMG (c). Bar = 50 μm (a and b) and 100 μm (c).

deposited solids obtained from thiirane–TMG mixtures (for $r = 1$ $Ge_{1.00}C_{2.30}$ $S_{1.22}O_{0.36}$ and for $r = 0.2$ $Ge_{1.00}C_{0.67}$ $S_{0.29}O_{0.30}$) is lower than it would correspond to relative depletion of both precursors (Fig. 1), which indicates that some portion of S was lost due to a reaction with atmosphere.

The FTIR spectra of the solids show very similar pattern and their comparison (Fig. 3) to that of the solid from thiirane and TMG is illustrated by using the spectrum of the solid obtained from TMG–thiirane ($r = 0.2$). The solid from TMG shows a typical pattern [9,12] of poly(carbogermane) at 2960–2899, 1410, 1232, 1040, 826, 780, 672 and 590 cm^{-1}, which are in the given order assignable to ν(C–H), $\delta^{as}(CH_3)$, $\delta^{s}(CH_3)$, $\nu(GeCH_2Ge)$, $\rho(CH_3)$ and ν(Ge–C) vibrations. The EDX analyses strongly suggest that the bands at 780 and 826 cm^{-1} are contributed by ν(Ge–O) vibrations [14]. The IR spectra of the solid from thiirane consist of bands at 2960, 1261, 1096, 1023, 803 and 670 cm^{-1} that are respectively due [15] to ν(C–H), skeletal ν(C–C), ν(C=S) and ν(S–C–X, X=C,X) vibrations. The spectra of the solids from TMG–thiirane mixtures possess all characteristic bands of the deposits obtained from the separate TMG and thiirane and they lack characteristic bands [16] of GeS (at 565–572 cm^{-1}) and GeS_2 (649–662 cm^{-1}).

These germanium sulfides are, however, detected by other, more sensitive techniques.

Thus, the Raman spectra show a typical pattern consisting of bands (A–F) at 298, 359, 600, 1040, 1243 and 1357 cm^{-1} which are, in the given order, assignable to the phonon band of Ge [17], β- and/or glassy GeS_2 [18], a local vibrational mode of C in Ge [19], ν(Ge–C–Ge), ν(C=S) [15c] and ν(C=C) vibrations. The representative spectrum is compared to those of the solid from thiirane and TMG in Fig. 4.

TEM images reveal the presence of nanostructured materials and show small bodies of about 10 nm-sized bodies agglomerated into large structures (Fig. 5).

Electron diffraction patterns of different selected regions (Fig. 6) show distances of synthetic GeS and Ge and confirm

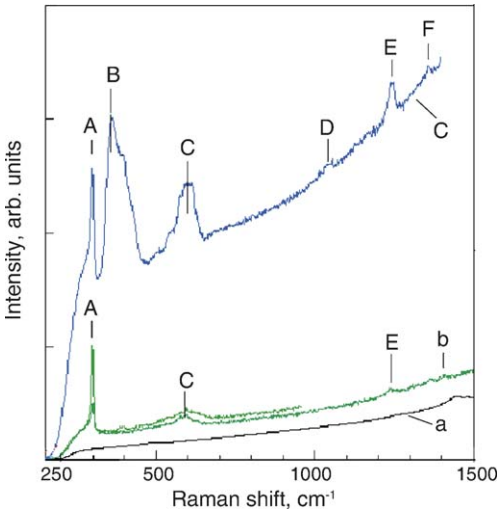

Fig. 4. Raman spectrum of the deposit from thiirane (a), TMG two different areas (b), and thiirane–TMG ($r = 0.5$) (c).

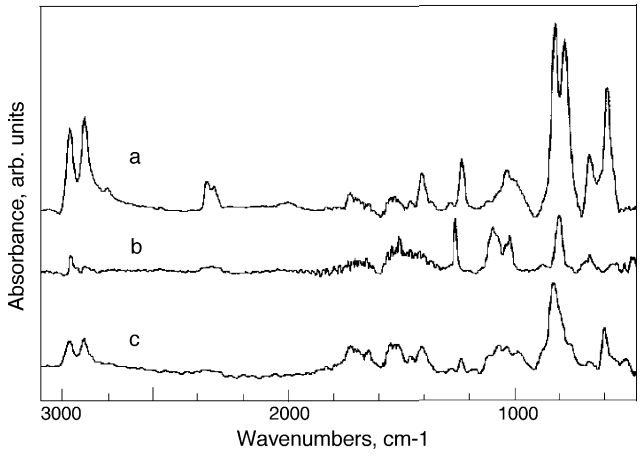

Fig. 3. FTIR spectrum of the solid from TMG (a), thiirane (b), and TMG–thiirane ($r = 0.2$) (c).

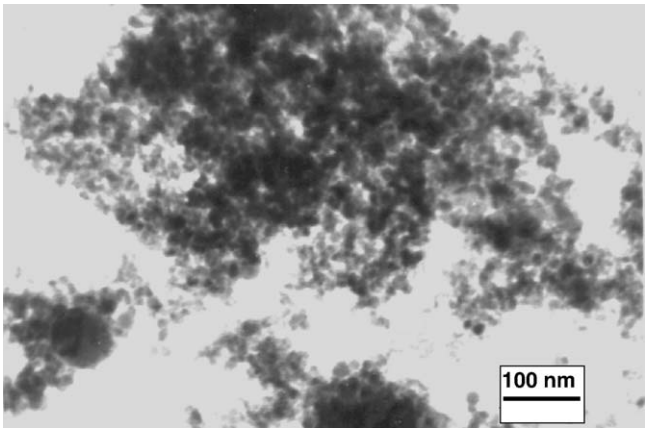

Fig. 5. Typical TEM image of the deposit obtained from thiirane–TMG mixture.

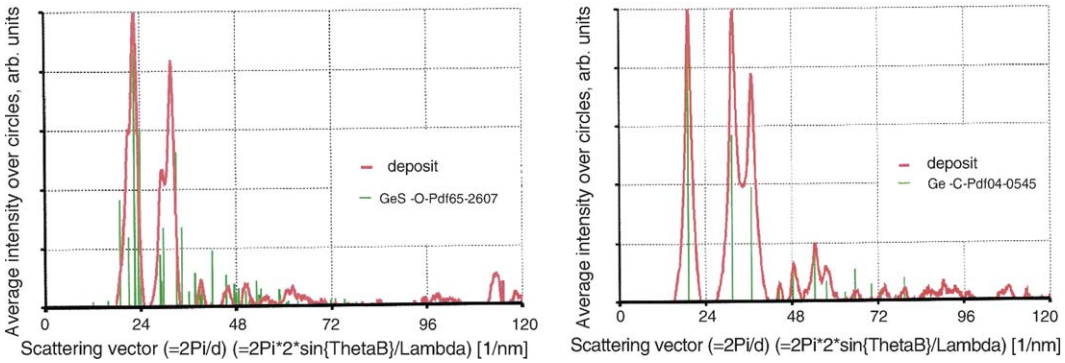

Fig. 6. The comparison of diffraction patterns of deposited solids and synthetic Ge and GeS (diffraction patterns from XRD diffraction database [11]).

good fits to interlayer distances of crystalline Ge and GeS phases. These analyses show that GeS and Ge are not equally distributed in the deposit and we give, for the sake of clarity, only patterns of deposit areas that show the presence of one of these constituents.

3.3. Gas-phase chemistry

We explain the formation of the germanium sulfides, the crystalline GeS and amorphous GeS_2, by a direct reaction between nanosized clusters of elemental germanium and sulfur. The Ge clusters are produced by the reported [9] decomposition steps of TMG (Ge–C homolysis and molecular elimination of methane and ethane) together with a poly(carbogermane). The S atoms are formed by the reported [8] elimination of S from thiirane together with a S-containing polymer. These steps are illustrated in Scheme 1.

We note that the formation of the poly(carbogermane) [12] is in keeping with transient occurrence and polymerization of Ge-containing radicals and species possessing the >Ge=CH_2 bond, and that that of the S-containing polymer involves association reactions of CS_2 and ethylene [20], insertion into C–H bond of S atoms [21] and addition of S atoms [22] and S-centered radicals [23] to double bonds of unsaturated intermediates. The assumed steps can interfere and lead to S-containing poly(carbogermanes) containing germathione [24] units. The observed oxygen incorporation can then be explained by reactions of Ge=S or Ge=CH_2 bonds with moisture [12] and/or by oxidation of Ge nanobodies with air [25].

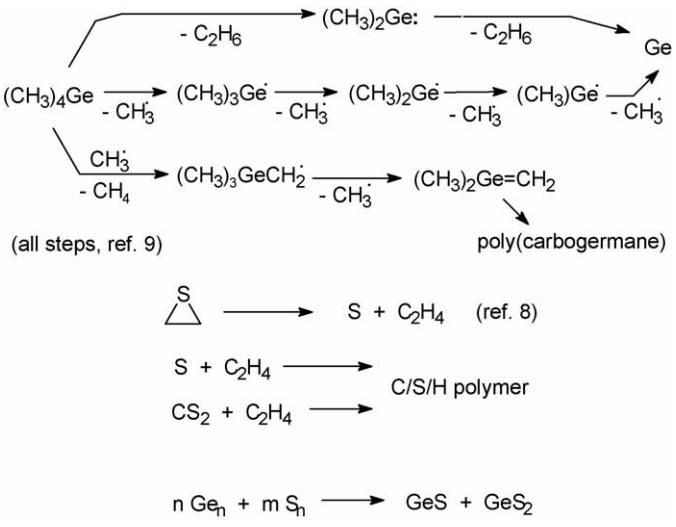

Scheme 1.

In conclusion, we point out that our data provide the first example of the reaction between elemental S and Ge in the gas phase kept at ambient temperature, leading to nano-sized germanium sulfides. They show that the products of this reaction are amorphous GeS_2 and crystalline GeS along with S- and Ge-containing polymers. The results extend our recent reports [4c,26] on laser-augmented formation of metal chalcogenides at ambient temperature of the reaction media.

Acknowledgement

This work was supported by grant ME486 (KONTAKT). R.T. was on leave from St. Cyril and Methodian University in Skopje.

References

[1] (a) T.B. Nasrallah, H. Dlala, M. Amlouk, S. Belgacem, C. Bernède, Synth. Met. 151 (2005) 225, and references therein;
(b) S.N. Sharma, R.K. Sharma, K.N. Sood, S. Singh, Mater. Chem. Phys. 93 (2005) 368, and references therein;
(c) T.B. Nasr, N. Kamoun, C. Guasch, Mater. Chem. Phys. 96 (2006) 84.
[2] (a) W. Qingqing, Z. Gaoling, H. Gaorong, Mater. Lett. 59 (2005) 2625, and references therein;
(b) T. Hirai, M. Ota, Mater. Res. Bull. 41 (2006) 19, and references therein.
[3] (a) S.-M. Lee, Y.-W. Jun, S.-N. Cho, J. Cheon, J. Am. Chem. Soc. 124 (2002) 11244;
(b) S. Chen, W.M. Liu, Mater. Chem. Phys. 98 (2006) 183.
[4] (a) S.-Y. Hong, R. Popovitz-Biro, Y. Prior, R. Tenne, J. Am. Chem. Soc. 125 (2003) 10470;
(b) X.-L. Gou, J. Chen, P.-W. Shen, Mater. Chem. Phys. 93 (2005) 557;
(c) R. Tomovska, V. Vorlíček, J. Boháček, J. Šubrt, J. Pola, New. J. Chem. 29 (2005) 785.
[5] M. Seki, K. Hachiya, K. Yoshida, J. Non-Cryst. Solids 315 (2003) 107, and references therein.
[6] (a) N. Suliţanu, Mater. Sci. Eng. B 83 (2001) 84;
(b) S. Rajagopalan, K.S. Harshavardhan, L.K. Malhotra, K.L. Chopra, J. Non-Cryst. Solids 50 (1982) 29.
[7] (a) J. Pola, D. Pokorná, M.J. Díanez, M.J. Sayagués, Z. Bastl, V. Vorlíček, Appl. Organometal. Chem. 19 (2005) 854;

(b) D. Pokorná, J. Boháček, V. Vorlíček, J. Šubrt, Z. Bastl, E.A. Volnina, J. Pola, J. Anal. Appl. Pyrol. 75 (2006) 65.
[8] (a) F. Qi, O. Sorkhabi, A.G. Suits, S.-H. Chien, W.-K. Li, J. Am. Chem. Soc. 123 (2001) 148;
(b) P. Felder, E.A.J. Wannenmacher, I. Wiedmer, J.R. Huber, J. Phys. Chem. 96 (1992) 4470;
(c) H.L. Kim, S. Satyapal, P. Brewer, R. Bersohn, J. Chem. Phys. 91 (1989) 1047.
[9] (a) J. Pola, R. Taylor, J. Organometal. Chem. 437 (1992) 271;
(b) J. Pola, J.P. Parsons, R. Taylor, J. Chem. Soc., Faraday Trans. 88 (1992) 1637.
[10] J.L. Lábár, in: L. Frank, F. Ciampor (Eds.), Proceedings of EUREM 12, Czechoslovak Society for Electron Microscopy, Brno, Czech Republic, 2000, p. 1379.
[11] Powder Diffraction File, Release 2000. PDF-2, International Centre for Diffraction Data; Newton Square, PA, USA.
[12] M. Lesbre, P. Mazerolles, J. Satgé, The Organic Compounds of Germanium, Wiley, London, 1971.
[13] E.M. Lown, H.S. Sandhu, H.E. Gunning, O.P. Strausz, J. Am. Chem. Soc. 90 (1968) 7164.
[14] (a) F. Glockling, The Chemistry of Germanium, Academic Press, London, 1969;
(b) V.C. Farmer, J.D. Russell, Spectrochim. Acta 18 (1962) 461.
[15] (a) Infrared Structural Correlation Tables and Data Cards, R.G.J. Miller, H.A. Willis, eds., Heyden & Son Ltd., Spectrum House, London, 1969;
(b) R. Tomovska, Z. Bastl, J. Pola, Macromol. Chem. Phys. 205 (2004) 2339, and references therein;
(c) R. Tomovska, Z. Bastl, V. Vorlíček, K. Vacek, J. Šubrt, Z. Plzák, J. Pola, J. Phys. Chem. B 107 (2003) 9793, and references therein.
[16] P. Hassanzadeh, L. Andrews, J. Phys. Chem. 96 (1992) 6181, and references therein.
[17] B.A. Weinstein, M. Cardona, Phys. Rev. B 7 (1973) 2545.
[18] Z. Černošek, E. Černošková, L. Beneš, J. Mol. Struct. 435 (1997) 193.
[19] J.C. Tang, K. Eberl, S. Zollner, S.S. Iyer, Appl. Phys. Lett. 61 (1992) 961.
[20] (a) R. Tomovska, M. Urbanová, R. Fajgar, Z. Bastl, J. Šubrt, J. Pola, Macromol. Rapid Commun. 25 (2004) 587;
(b) R. Tomovska, Z. Bastl, J. Pola, Macromol. Chem. Phys. 205 (2004) 2339.
[21] M.L. McKee, J. Am. Chem. Soc. 108 (1986) 5059.
[22] K.S. Sidhu, E.M. Lown, O.P. Strausz, H.E. Gunning, J. Am. Chem. Soc. 88 (1966) 254.
[23] (a) R.J. Balla, B.R. Weiner, H.H. Nelson, J. Am. Chem. Soc. 109 (1987) 4804;
(b) C. Anastasi, M. Broomfield, O.J. Nielsen, P. Pagsberg, Chem. Phys. Lett. 182 (1991) 643.
[24] J. Escudié, C. Conset, H. Ranaiovonjatoro, J. Satgé, Coord. Chem. Rev. 130 (1994) 427.
[25] T. Hanrath, B.A. Korgel, J. Am. Chem. Soc. 126 (2004) 15466.
[26] (a) A. Ouchi, Z. Bastl, J. Boháček, H. Orita, K. Miyazaki, S. Miyashita, P. Bezdička, J. Pola, Chem. Mater. 16 (2004) 3439;
(b) J. Pola, D. Pokorná, M.J. Diánez, M.J. Sayagués, Z. Bastl, V. Vorlíček, Appl. Organometal. Chem. 19 (2005) 854.